V European Conference on Computational Fluid Dynamics
ECCOMAS CFD 2010
J. C. F. Pereira and A. Sequeira (Eds)
Lisbon, Portugal,14-17 June 2010

SYMMETRY-PRESERVING REGULARIZATION OF THE NAVIER-STOKES EQUATIONS

R.W.C.P. Verstappen[*] and F.X. Trias[†]

[*]Johann Bernoulli Institute for Mathematics and Computer Science,
University of Groningen
P.O. Box 407, 9700 AK Groningen, The Netherlands
r.w.c.p.verstappen@rug.nl
[†]Centre Tecnològic de Transferència de Calor (CTTC) ETSEIAT,
Technical University of Catalonia
c/Colom 11, 08222 Terrassa, Spain
xavi@cttc.upc.edu

Key words: Large-eddy simulation, regularization modeling, turbulence, heat transfer, differentially heated cavity

Abstract. *The Navier-Stokes equations accurately describe turbulent flow, yet they do not provide a tractable model. Typically, the range of scales of motion is so wide that in the foreseeable future numerical simulations of turbulent flow have to resort to models accounting for the effects of the small scales of motion for which numerical resolution is not avaliable. At the crossroad of theory and numerical simulation new tractable models for turbulence start to develop. Regularization models form an example thereof. The regularization method basically alters the nonlinearity to control the convective energetic exchanges. The first outstanding approach in this direction goes back to Leray. In this paper, we consider regularization that preserve certain fundamental properties of (the convective operator in) the Navier-Stokes equations exactly. More precisely, we discuss regularizations that preserve the symmetry and conservation properties of the convective operator. The underlying idea is to restrain the convective production of small scales in an unconditional stable manner, meaning that the solution of the regularized system cannot blow up in the energy norm. The numerical algorithm used to solve the governing equations preserves the symmetry properties too and is therefore well-suited to test the proposed simulation shortcut. The simulation shortcut is successfully tested for turbulent natural convection in a differentially heated cavity.*

1 Introduction

Turbulent flow can be visualized as a cascade of energy from large to small scales of motion. The energy introduced at the large scales is transferred to smaller and smaller scales - nearly without viscous dissipation - until the scale becomes sufficiently small to dissipate energy efficiently. The Navier-Stokes equations provide an appropriate model for turbulent flow. In the absence of compressibility ($\nabla \cdot u = 0$), the equations are

$$\partial_t u + C(u,u) + D(u) + \nabla p = 0, \tag{1}$$

where u denotes the instantaneous fluid velocity field, and p stands for the pressure. The linear term $D(u) = -\Delta u/\mathrm{Re}$ is dissipative; Re is the Reynolds number. The dissipative operator D is the most effective at the smallest scales of motion. The nonlinear term $C(u,v) = (u \cdot \nabla)v$ transfers energy from the scales at which the flow is driven to the smallest ones that survive dissipation. The entire range of scales of motion is to be resolved when turbulence is computed directly from the Navier-Stokes equations. Consequently, attempts at simulating turbulence directly are limited to "a milli-second over a postage stamp" [1].

In most applications it suffices to have a good grasp of the large scales of motion. Resolving only these primary features of the flow reduces the computational effort to a feasible level. Therefore a coarse-grained description of turbulent flow is sought. In large-eddy simulation (LES) the coarsened representation is based on scale separation. To that end a spatial filter is introduced. Applying this filter to the Navier-Stokes equations yields the following equation for the 'large-eddies',

$$\partial_t \overline{u}_\epsilon + C(\overline{u}_\epsilon, \overline{u}_\epsilon) + D(\overline{u}_\epsilon) + \nabla \overline{p}_\epsilon = C(\overline{u}_\epsilon, \overline{u}_\epsilon) - \overline{C(u_\epsilon, u_\epsilon)} \approx M(\overline{u}_\epsilon), \tag{2}$$

where the filtering operation is denoted by a bar; the width of the filter is given by ϵ. The right-hand side in the equation above represents the effects of the residual scales on the evolution of the filtered velocity field. This nonlinear term is to be modeled. Here the model is denoted by $M(\overline{u}_\epsilon)$. LES-models are often based on phenomenological arguments that cannot be derived from the Navier-Stokes equations [2].

In the quest for a dynamically less complex mathematical formulation, we consider smooth approximations (regularizations) of the nonlinearity:

$$\partial_t u_\epsilon + \widetilde{C}(u_\epsilon, u_\epsilon) + D(u_\epsilon) + \nabla p_\epsilon = 0. \tag{3}$$

The regularized system (3) should be more amenable to solve numerically, while the leading modes of u_ϵ have to approximate the corresponding modes of the Navier-Stokes solution u. The first outstanding approach in this direction goes back to Leray [3], who took $\widetilde{C}(u,u) = C(\bar{u},u)$ and proved that any filtering of the transport velocity is sufficient to guarantee that the energy cascade stops at a certain scale of motion. Cheskidov *et al.* [4] have showed that the complexity of the dynamics given by the 3D Leray model

lies between that of the 2D and 3D Navier-Stokes equations. The Navier-Stokes-α-model forms another example of regularization modeling [5]. In this model, the convective term becomes $\widetilde{C}_r(u,u) = C_r(u,\bar{u})$, where C_r denotes the convective operator in rotational form: $C_r(u,v) = (\nabla \times u) \times v$.

In case an invertible filter is applied (the Gaussian filter, for instance), the regularization (3) falls in with the LES-concept if the subgrid model $M(\overline{u}_\epsilon)$ is taken such that

$$M(\overline{u}_\epsilon) = C(\overline{u}_\epsilon, \overline{u}_\epsilon) - \overline{\widetilde{C}(u_\epsilon, u_\epsilon)} \tag{4}$$

Indeed under this condition, Eq. (3) is equivalent to (2): we can filter (3) first and thereafter compare the filtered version of (3) term-by-term with (2) to identify the closure model $M(\overline{u}_\epsilon)$. Eq. (4) relates the regularization $\widetilde{C}(u_\epsilon, u_\epsilon)$ one-to-one to the closure model for any invertible filter. Hence, Eq. (3) is formally equivalent to a LES for any invertible filter. The regularization (3) may also be seen in relationship to the approximate deconvolution method (ADM) [6]. In ADM, the argument u in the bilinear operator $\overline{\mathcal{C}(u,u)}$ is replaced by $\widetilde{u} = \widetilde{\mathcal{F}}^{-1}\overline{u} \approx u$, where $\widetilde{\mathcal{F}}^{-1}$ approximates the inverse of the filter $\mathcal{F}u = \overline{u}$. The approximately deconvolved velocity is then governed by

$$\partial_t \widetilde{u} + \widetilde{\mathcal{F}}^{-1}\mathcal{F}\mathcal{C}(\widetilde{u},\widetilde{u}) + \mathcal{D}(\widetilde{u}) + \nabla\widetilde{p} = 0.$$

Taking $\widetilde{u} = u_\epsilon$, $\widetilde{p} = p_\epsilon$ and $\widetilde{\mathcal{C}}(u,v) = \widetilde{\mathcal{F}}^{-1}\mathcal{F}\mathcal{C}(u,v)$ yields Eq. (3). In this way, any direct modification of the convective term in the Navier-Stokes equations is implicitly related to an approximate deconvolution operator $\widetilde{\mathcal{F}}^{-1}$.

The regularization method basically alters the nonlinearity to restrain the production of small scales of motion, see e.g. [7]. In doing so, one can preserve certain fundamental properties of the convective operator in the Navier-Stokes equations exactly. We propose to preserve the symmetry properties that are intimately tied up with the conservation of energy, enstrophy (in 2D) and helicity.

2 Symmetry and conservation properties

In terms of the usual scalar product $(u,v) = \int_\Omega u \cdot v dx$, the energy of a fluid occupying a region Ω is given by $|u|^2 = (u,u)$. The evolution of the energy follows from differentiating (u,u) with respect to time and rewriting $\partial_t u$ with the help of (1). In this way, we get a convective contribution given by $(C(u,u),u)$. The trilinear form $(C(u,v),w)$ is skew-symmetric with respect to v and w:

$$(C(u,v),w) = -(v,C(u,w)) \tag{5}$$

provided $\int_{\partial\Omega}(v\cdot w)(u\cdot n)ds = 0$; *e.g.*, if the normal velocity $u\cdot n$ vanishes at the boundary $\partial\Omega$, if $v\cdot w$ vanishes, or if periodic boundary conditions apply. The proof of (5) uses the identity $\nabla\cdot(fu) = f\nabla\cdot u + \nabla f\cdot u$, which holds for any (differentiable) scalar f and

vector field u. Taking $f = v \cdot w$, $\nabla \cdot u = 0$ and applying Gauß's Divergence Theorem gives $(C(u,v) \cdot w) + (C(u,w) \cdot v) = (\nabla f \cdot u) = (\nabla \cdot (fu)) = 0$, which proves (5).

Eq. (5) demonstrates that the convective contribution $(C(u,u),u)$ cancels from the energy equation. The pressure does not contribute. Thus after some algebra, the energy equation reduces to

$$\frac{\mathrm{d}}{\mathrm{d}t}\tfrac{1}{2}|u|^2 = -\tfrac{1}{\mathrm{Re}}|\nabla u|^2 = -\tfrac{1}{\mathrm{Re}}|\omega|^2, \tag{6}$$

where $\omega = \nabla \times u$ is the vorticity. This shows that the enstrophy $|\omega|^2$ determines the rate of dissipation of energy. Taking the curl of the Navier-Stokes equations gives

$$\partial_t \omega + C(u,\omega) + D(\omega) = C(\omega,u), \tag{7}$$

Consequently, the enstrophy is governed by

$$\frac{\mathrm{d}}{\mathrm{d}t}\tfrac{1}{2}|\omega|^2 = -\tfrac{1}{\mathrm{Re}}|\nabla \omega|^2 + (C(\omega,u),\omega). \tag{8}$$

The trilinear term in (8) vanishes in two spatial dimensions; hence, the enstrophy is conserved in 2D (if $\mathcal{D} = 0$). This property is extensively used in the proof of the existence and uniqueness of (weak and strong) solutions of the 2D Navier-Stokes equations. In 3D, however, $(C(\omega,u),\omega) \neq 0$ and the question of existence and uniqueness is still open. At the present level of understanding, it cannot be excluded that the vorticity ω bursts driving the energy to extreme small scales by the vortex stretching mechanism.

The evolution of the helicity (ω,u) follows from the inner product of Eq. (1) with the vorticity ω and the inner product of Eq. (7) with the velocity u. Taking these inner products results into the convective contribution $(C(u,u),\omega) + (C(u,\omega),u) - (C(\omega,u),u)$, which vanishes as an immediate consequence of the skew symmetry (5). Thus, the helicity is conserved (if $D = 0$).

3 Symmetry-preserving regularizations

Regularizations of particular interest conserve the energy, the enstrophy (in 2D) and the helicity (in 3D) in the absence of viscous dissipation. The Leray model conserves the energy, but not the enstrophy or helicity, whereas the Navier-Stokes-α model conserves the enstrophy and helicity, yet not the energy. Since the invariance of energy, enstrophy and helicity is intimately tied up with the symmetry properties of the convective operator $\mathcal{C}$ (see Section 2), we aim to approximate $\mathcal{C}$ in such manner that the skew-symmetry given by Eq. (5) is preserved. This criterion yields the following class of approximations

$$\partial_t u_\epsilon + \widetilde{C}_n(u_\epsilon,u_\epsilon) + D(u_\epsilon) + \nabla p_\epsilon = 0, \tag{9}$$

$(n = 2,4,6)$ in which the convective term is approximated according to:

$$\widetilde{C}_2(u,v) = \overline{C(\overline{u},\overline{v})} \tag{10}$$

$$\widetilde{C}_4(u,v) = C(\overline{u},\overline{v}) + \overline{C(\overline{u},v')} + \overline{C(u',\overline{v})} \tag{11}$$

$$\widetilde{C}_6(u,v) = C(\overline{u},\overline{v}) + C(\overline{u},v') + C(u',\overline{v}) + \overline{C(u',v')} \tag{12}$$

where a prime indicates the residual of the filter, *e.g.* $u' = u - \overline{u}$. The difference between $\widetilde{C}_n(u,u)$ and $C(u,u)$ is of the order ϵ^n (where n=2,4,6) for symmetric filters with filter length ϵ. The nonlinear approximations (10)-(12) are constructed in such a manner that the skew-symmetry (5) is preserved. That is, for any self-adjoint filter:

$$(\widetilde{C}_n(u,v),w) = -(v,\widetilde{C}_n(u,w)), \tag{13}$$

with $n = 2, 4, 6$. Eq. (13) implies that the convective contribution to the energy equation vanishes. Consequently, the evolution of the energy $\frac{1}{2}|u_\epsilon^2|$ of any solution u_ϵ of (9)-(12) is again given by Eq. (6) with u replaced by u_ϵ.

4 Nonlinear transport mechanism

To see how the above regularizations restrain the production of small scales of motion, we take the curl of Eq. (9),

$$\partial_t \omega_\epsilon + \widetilde{C}_n(u_\epsilon,\omega_\epsilon) + D(\omega_\epsilon) = \widetilde{C}_n(\omega_\epsilon,u_\epsilon).$$

This equation resembles the vorticity equation that follows from the Navier-Stokes equations: the only difference is that C is replaced by its regularization $\widetilde{C}_n$. The Navier-Stokes equations yield the vortex-stretching term

$$C(\omega,u) = \overline{S}\overline{\omega} + \overline{S}\omega' + S'\overline{\omega} + S'\omega,$$

where $S = \frac{1}{2}(\nabla u + \nabla u^{\mathrm{T}})$ is the deformation tensor. The regularized vortex stretching terms become

$$\begin{aligned} C_2(\omega,u) &= \overline{\overline{S}\overline{\omega}} \\ C_4(\omega,u) &= \overline{S}\overline{\omega} + \overline{\overline{S}\omega'} + \overline{S'\overline{\omega}} \\ C_6(\omega,u) &= \overline{S}\overline{\omega} + \overline{S}\omega' + S'\overline{\omega} + \overline{S'\omega'}, \end{aligned}$$

respectively. Qualitatively, vortex stretching leads to the production of smaller and smaller scales, *i.e.*, to a continuous, local increase of both S' and ω'. Consequently, at the positions where vortex stretching occurs, the terms with S' and ω' will eventually amount considerably to $C(\omega,u)$. Since the regularizations $C_n(\omega,u)$ diminish these terms, they counteract the production of smaller and smaller scales by means of vortex stretching and may eventually stop the continuation of the vortex stretching process. In this way, the symmetry-preserving regularization method restrains the convective production of smaller and smaller scales of motion by means of vortex stretching.

A detailed study of the triadic interactions shows that $\widetilde{C}_n(u,u)$ approximates the local interactions between large scales of motion ($\epsilon|k| < 1$) up to n-th order. Hence, the triadic interactions between large scales of motion are only slightly altered. All interactions involving longer wavevectors (smaller scales of motion) are reduced. The amount by which

the interactions between the wavevector-triple (k, p, q) are lessened depends on the length of the legs of the triangle $k = p + q$. In case $n = 4$, for example, all triadic interactions for which at least two legs are (much) longer than $1/\epsilon$ are (strongly) attenuated, whereas interactions for which at least two legs are (much) shorter than $1/\epsilon$ are reduced to a small degree only. For more details, see [8]

5 Mathematical basis

The symmetry-preserving regularizations (9)-(12) yield uniqueness and the expected regularity properties: for all initial velocities in $H = \{u \in \mathrm{L}^2(\Omega), \nabla \cdot u = 0\}$ where the spatial domain is given by $\Omega = (0, 2\pi)^3$ and periodic boundary conditions are enforced, and $\epsilon > 0$, Eq. (9), with $\mathcal{C}_n$ given by (10)-(12), has a unique C^∞ solution. This solution is bounded in $L^\infty(0, T; H) \cap L^2(0, T; V)$, where the time $t \in (0, T)$, with $T > 0$ arbitrary, and $V = \{u \in \mathrm{H}^1(\Omega), \nabla \cdot u = 0\}$). One subsequence converges weakly in $L^2(0, T; V)$ to a weak NS-solution as $\epsilon \to 0$. The proof is in fact a copy of Leray's proof in [3]. So as for Leray's model, any filtering in Eqs. (10)-(12) is sufficient to guarantee that the energy cascade stops at a certain scale of motion.

Fifty years after Kolmogorov's landmark papers on the cascade-concept [9]-[10], Foias et al. [11] proved Kolmogorov's results in a mathematically rigorous manner. They proved that the solution (existence is assumed) of the NS-equation - on a periodic box in dimension three - actual has a range of scales with wavenumber κ for which the rate at which energy is transferred (from scales $> \kappa$ to those $< \kappa$) is independent of κ. In this range the energy behaves like $\kappa^{-5/3}$. The proofs by Foias et al. are also applicable to the regularized system (9), because the regularization preserves symmetry and conservation properties of the nonlinearity. In this way it can be shown that the solution of the regularized system - on a periodic box in dimension three - actual has a range of scales with wavenumber k for which the rate at which energy is transferred (from scales $> k$ to those $< k$) is independent of k [12]. In this so-called inertial subrange the energy behaves like $k^{-5/3}$. Compared to Navier-Stokes, the inertial subrange is shortened yielding a more amenable problem to solve numerically.

6 Numerical simulation method

The discretization of Eq. (9) is important, since modelling errors and discretization errors are mixed together if results computed with the help of (9) are compared with reference data. The approximations $\mathcal{C}_n$ of $\mathcal{C}$ are constructed such that the symmetry property given by Eq. (5) is preserved. Of course, the same should hold for the spatial discretization of $\mathcal{C}_n$. Therefore, we have developed a discretization scheme that preserves the skew-symmetry of the convective term. For more details the reader is referred to [13].

7 Results for a turbulent DHC at Ra = 10^{10}

The performance of the C_4-approximation has been tested for a turbulent differentially heated cavity (DHC) by direct comparison with the DNS reference results [14, 15, 16]. The coordinate system used here is: x_1 for the periodic direction and x_2 (horizontal) and x_3 (vertical) for the two wall-normal directions (see Figure 1, left). Ra is the Rayleigh number based on the cavity height, $(g\beta\Delta T L_3^3)/(\nu\alpha)$ and $Pr = \nu/\alpha$. To account for the density variations, the Boussinesq approximation is used. Furthermore, the cavity is filled with air ($Pr = 0.71$), and its height aspect ratio, L_3/L_2, is equal to 4. For further details about this configuration the reader is referred to [14, 15, 16]

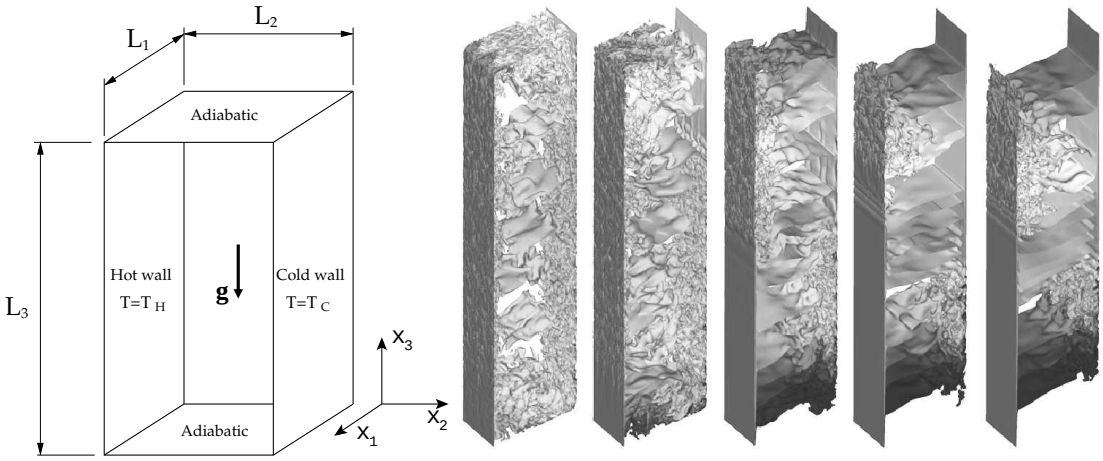

Figure 1: Differentially heated cavity schema. Right: Several instantaneous temperature fields.

Averages over the three statistically invariant transformations (time, x_1-direction and central point symmetry around the center of the cavity) have been carried out. The standard averaging notation, $\langle\cdot\rangle$, is used here. Statistical values have been obtained for a time interval corresponding to ≈ 500 time units of simulation. As initial test, two very coarse meshes (see Table 1) have been used to solve the DHC-problem at $Ra = 10^{10}$.

7.1 Mean fields

The corresponding vertical temperature profile at mid-width is displayed in Figure 2. At first sight we can observe a significant improvement for the smoothed solutions. At the top and bottom areas, where the flow is more turbulent, some discrepancies regarding the reference solution are still observed for both meshes. The fairly good prediction at the cavity core even for the coarsest mesh is especially relevant. Actually, an accurate prediction of thermal stratification of this configuration is a challenge for turbulence modeling. In Figure 3 (top), we can see that without smoothing ($\epsilon = 0$), the thermal stratification is clearly under predicted, especially for the coarsest mesh.

Let us focus now on the vertical boundary layer. It remains laminar in its upstream

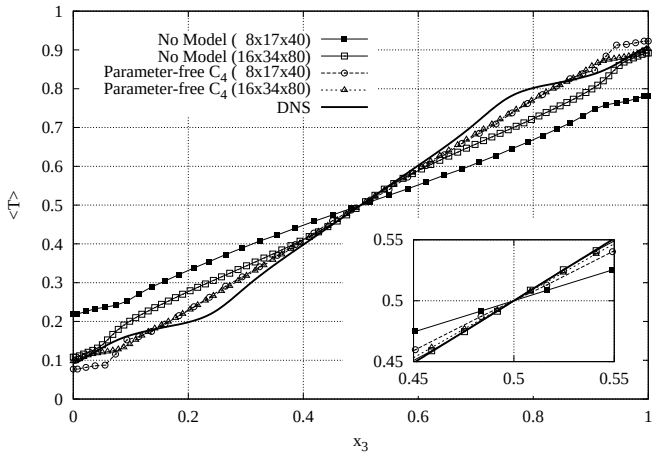

Figure 2: Averaged vertical temperature profile at mid-width.

part up to the point where the Tollmien-Schlichting waves travelling downstream grow up enough to disrupt the boundary layer (see Figure 1, right). Its high sensitivity to external disturbances makes it difficult to predict. The corresponding temperature and vertical velocity profiles at the cavity mid-height plane, $x_3 = 0.5$, are displayed in Figure 3. As expected, we can observe a strong relation between $\langle T \rangle$ and $\langle u_3 \rangle$. Consequently, both are to be predicted well. The solutions corresponding to $\epsilon = 0$ (labeled 'No Model') have a vertical boundary layer that is too thick, whereas with the C_4-smoothing, results for the two coarse meshes agree very well with the DNS reference solution.

7.2 Heat transfer

The total Nusselt numbers are shown in Table 1. The reference value $Nu = 101.94$ has been obtained from our DNS simulation [15, 16] with $\epsilon = 0$. We see that both C_4 simulations, RM1 and RM2 , predict fairly well the reference value. Moreover, in Figure 5, we observe that the heat transfer is also well captured for all randomly generated meshes whereas the solutions obtained without smoothing ($\epsilon = 0$) are incomparably worse. Results of the distribution of Nusselt number in the hot wall are shown in Figure 4. A change in the shape is observed at nearly $x_3 = 0.2$ for the non-smoothed results, indicating a much too early transition toward turbulence. In contrast, the C_4 results are able to capture well most of the profile except for the most upstream part where the heat transfer is slightly under predicted.

In Table 1, the maximum and the minimum values of the local Nusselt number are also shown. These two quantities are of interest because they occur in two clearly different parts of the vertical boundary layers. Maximum values occur in the upstream part of the boundary layer where it is still almost laminar whereas minimum values are observed at the most downstream part of the boundary layer where it has become fully turbulent. For both coarse grids, the significant improvements are achieved for the regularized solutions.

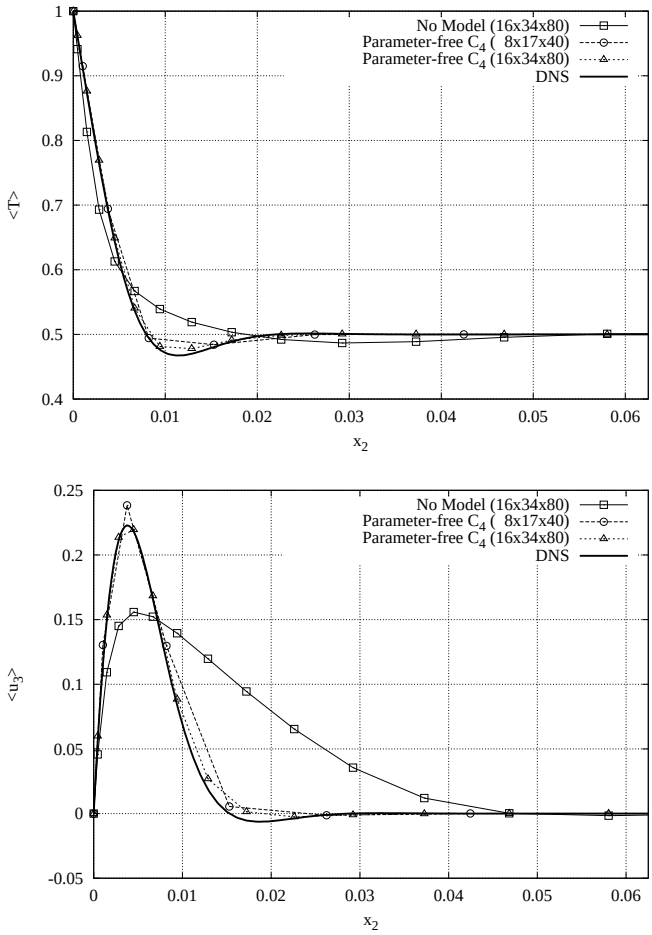

Figure 3: Averaged temperature (top) and vertical velocity (bottom) profiles at the horizontal mid-height plane.

	DNS	RM1		RM2	
Mesh	$128 \times 190 \times 462$	$16 \times 34 \times 80$		$8 \times 17 \times 40$	
		No model	C_4	No model	C_4
Nu	101.94	121.93	100.81	128.14	102.17
Nu_{max}	454.86	437.78	451.12	342.02	459.59
Nu_{min}	8.50	10.92	10.18	27.77	7.03

Table 1: The overall, the maximum and the minimum of the averaged Nusselt number.

7.3 Grid (in)dependence analysis

A reliable modeling of turbulence at (very) coarse grids is a great challenge. The coarser the grid, more convincing model quality is perceived. However, it might happen

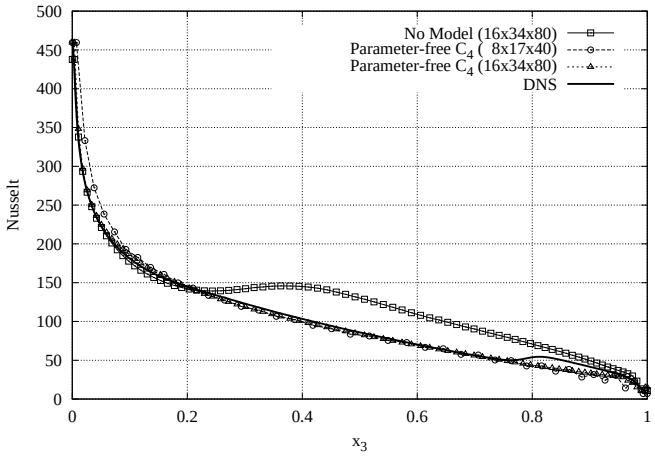

Figure 4: Local Nusselt number distribution.

that the solution is strongly dependent on meshing parameters and thus some particular combinations could 'accidentally' provide good results. An example of this behavior has been observed in [17] for a turbulent channel flow. In order to elucidate this point, the same DHC problem has been solved on a series of 50 randomly generated meshes: with (N_1, N_2, N_3)-values limited by those given by meshes RM1 and RM2 (see Table 1), *i.e.*, $8 \leq N_1 \leq 16$, $17 \leq N_2 \leq 34$, and $40 \leq N_3 \leq 80$. The concentration parameters are kept equal to those used for the DNS simulation [14]. Note than some of the numerical experiments displayed in Figure 5 correspond to highly skewed grids. Results for the overall Nusselt and the centerline stratification values are displayed in Figure 5 (top). At first sight, we can observe that the C_4 modeling predicts results well irrespective of the meshing whereas very poor and dispersed results are obtained when the model is switched off. The fairly good prediction of the stratification (note the dispersion obtained without model!) is especially important. Results for the maximum vertical velocity and the wall shear stress scaled at the horizontal mid-height plane, $x_3 = 0.5$, display essentially the same (see Figure 5, bottom).

8 Performance at higher (and lower) Rayleigh numbers

The performance of the C_4-regularization has also been tested at higher (and lower) Ra. This study covers a relatively wide range, $6.4 \times 10^8 \leq Ra \leq 10^{11}$, from weak to fully developed turbulence. Within this range DNS results for five different configurations (at $Ra = 6.4 \times 10^8$, 2×10^9, 10^{10}, 3×10^{10} and 10^{11}, respectively) are available [15, 16]. The meshes used to carry out these simulations have been generated keeping the same number of points in the boundary layer as in the coarse mesh RM1 for $Ra = 10^{10}$. In this way, the meshes[1] for $Ra = 3 \times 10^{10}$ and 10^{11} become $10 \times 19 \times 46$ with $\gamma_2 = 2.26$ and $12 \times 26 \times 62$ with $\gamma_2 = 2.28$, respectively.

[1]Note that the grid stretching near the vertical walls has also been slightly increased with the Ra.

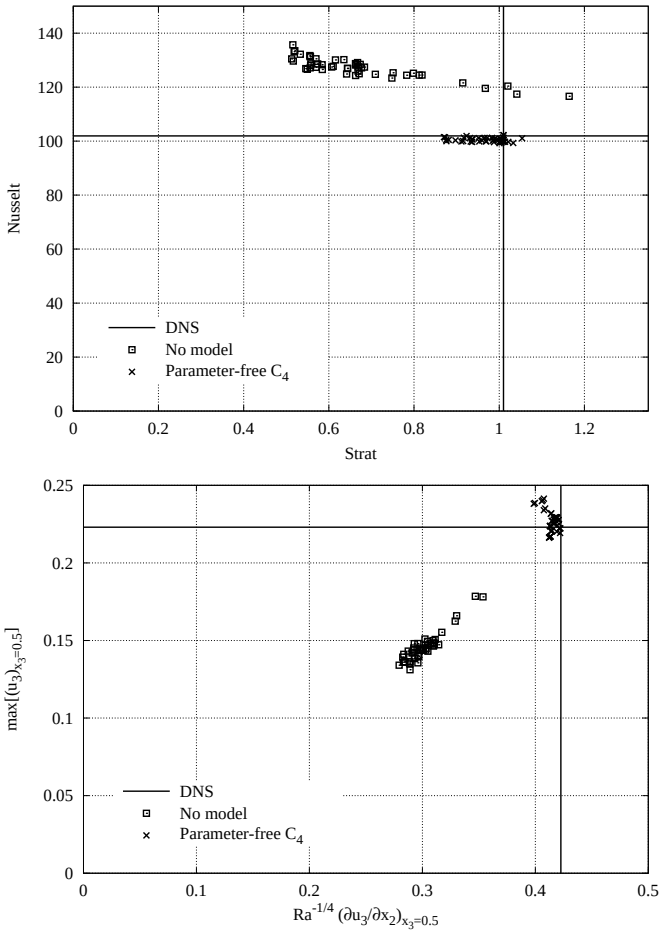

Figure 5: Top: the overall Nusselt number and the centerline stratification. Bottom: the maximum vertical velocity and the wall shear stress scaled by $Ra^{-1/4}$ at the horizontal mid-height plane. Results have been obtained for 50 randomly generated grids.

8.1 Boundary layer

For the sake of brevity, in this section we focus only on the highest Ra, *i.e.* 10^{11}. In Figure 6, the temperature and the vertical velocity profiles at the horizontal mid-height plane, $x_3 = 0.5$, are displayed. Again, the C_4 method and non-smoothed results ($\epsilon = 0$) obtained using a mesh that it is twice finer in each direction are compared with DNS data. All plots depict essentially the same: the C_4 method is able to capture well the flow structure of the vertical boundary layer even for the coarsest meshes whereas the results of the non-smoothed simulations differ largely from the reference solution.

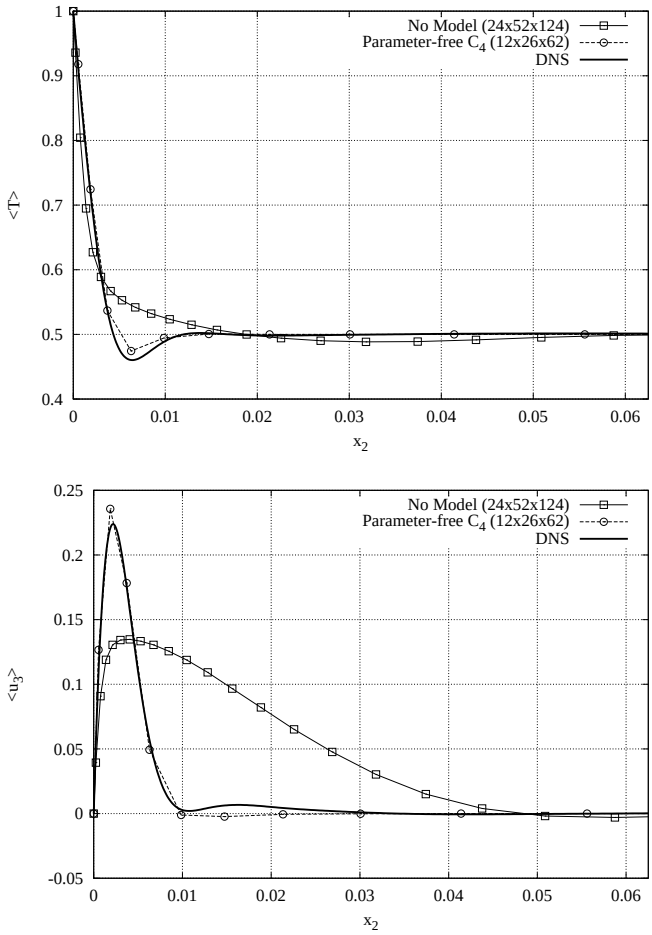

Figure 6: Averaged temperature (top) and vertical velocity (bottom) profiles at the horizontal mid-height plane at $Ra = 10^{11}$.

8.2 Heat transfer

The heat flux as a function of Rayleigh number is investigated in this section. In the last decades significant efforts, both numerical and experimentally, have been directed at investigating the mechanisms and detailed scaling behavior on turbulent Rayleigh-Bénard (RB) problems. Classical theory predicts that $Nu \sim Ra^{\xi}$ with $\xi = 1/3$. Alternative scaling theories, encouraged by experimental observations, lead to $\xi = 2/7$ [18]. Finally, an asymptotic regime, the so-called Kraichnan regime, with $\xi = 1/2$ is presumed to exist at very high Ra. Experimentally, power-law dependencies of heat flux with exponents between $1/4$ and $1/3$ have been measured [19]. Regarding the Kraichnan regime, and despite the great efforts devoted, no clear evidence has been observed yet [20]. On the other hand, there is still controversy whether a simple power-law $Nu \sim Ra^{\xi}$ is adequate [19]. Comparatively, the DHC problem has received much less attention from the scientific

community. Nevertheless, both configurations share similar heat transfer scaling [21] and most of the ideas applied to RB configuration can be easily applied to the DHC problem. In [16] we found that $Nu \approx 0.182 Ra^{0.275}$ was the power-law scaling that fitted best our DNS results in the range $Ra = 10^9 - 10^{11}$. Actually, this exponent cannot be considered 'near' 1/3; rather, it is closer to the $2/7 \approx 0.286$ proposed by alternatives theories of turbulent natural convection flows [18].

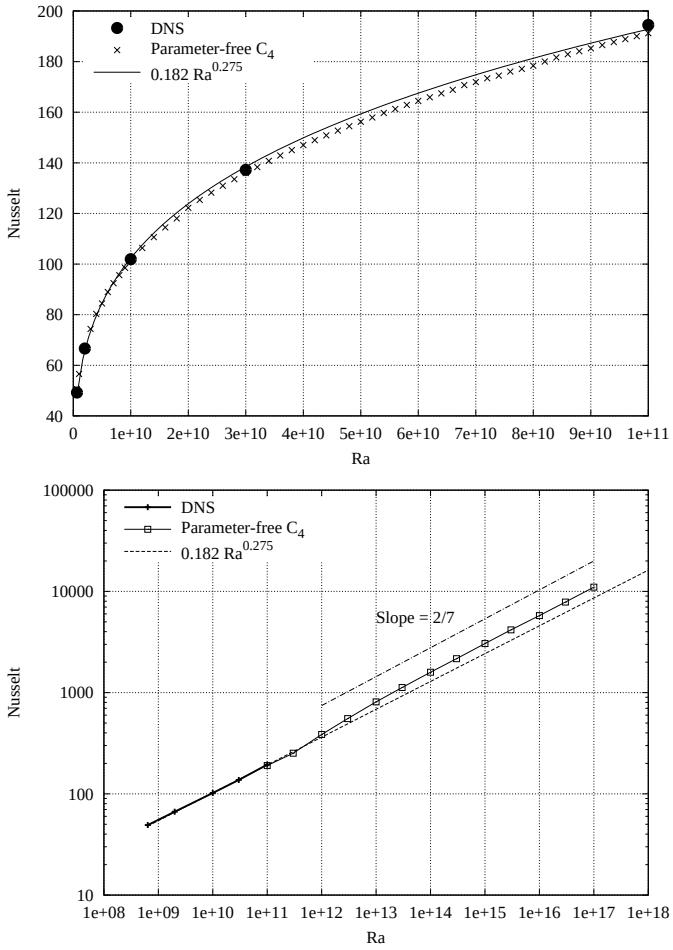

Figure 7: Overall Nusselt number for $6.4 \times 10^8 \leq Ra \leq 10^{11}$ (top) and for Ra up to 10^{17} (bottom).

8.2.1 Comparison with DNS results

Results for the overall Nusselt number corresponding to 56 simulations within the whole range of Rayleigh numbers studied by DNS, *i.e.*, $6.4 \times 10^8 \leq Ra \leq 10^{11}$, are displayed in Figure 7 (top). At first sight, we observe again a fairly good agreement with the DNS results (solid dots) and the correlation obtained from the DNS data. It must be noted

that the Nu-Ra dependence obtained with the C_4 is smooth suggesting again that the proposed model is performing well 'independently' of Ra and meshing parameters that may suddenly change for two consecutive points in the graph.

8.2.2 Nu-number correlation with Ra up to 10^{17}

Since performing computations with the C_4 approximation is rather cheap simulations at very high Ra have also been performed. Following the aforesaid criteria to keep the number of point at the vertical boundary layer constant leads to a $68 \times 142 \times 334$ mesh with $\gamma_2 = 3.48$ for $Ra = 10^{17}$. Of course, for the range $10^{11} < Ra \leq 10^{17}$ there is no DNS (or experimental) data to compare with. Anyhow, it is interesting to see that results displayed in Figure 7 (bottom) show a good agreement with a 2/7 power-law scaling of Nusselt (Nu increases approximately from 10^2 to 10^4, that is 2 orders of magnitude, when Ra is increased 7 orders, from 10^{10} to 10^{17}). This scaling law, predicted by alternatives theories [18] of turbulent natural convection, has also been experimentally measured for RB configurations [20].

9 Concluding remarks

The C_4-regularization of the nonlinear convective term has been considered as a simulation shortcut. The symmetries and conservation properties of the original convective term are exactly preserved. Doing so, the production of smaller and smaller scales of motion is restrained in an unconditionally stable manner. The numerical algorithm to solve the governing equations is also fully-conservative and is therefore well-suited to test the proposed simulation method.

An air-filled DHC with height aspect ratio 4 has been used as test case for the C_4-regularization. This is a challenging configuration for turbulence modeling since areas with completely different regimes coexist and interplay. Direct comparison with DNS reference results within a relatively wide range of Rayleigh numbers, $6.4 \times 10^8 \leq Ra \leq 10^{11}$, has shown that the method is able to capture the general pattern of the flow correctly even for very coarse meshes. The robustness of the method has been tested by performing simulations for a series of randomly generated grids. Even for highly skewed grids, all the results obtained with the $\mathcal{C}_4$ method were clustered around the DNS reference solution. Finally, to study the heat transfer scaling, simulations at higher Ra up to 10^{17} have also been computed. A fairly good agreement with a 2/7 power-law scaling of Nusselt has been measured for the whole range, *i.e.*$10^{11} \leq Ra \leq 10^{17}$. This scaling law, also predicted by alternatives theories of turbulent natural convection, has also been experimentally measured for RB configurations.

We can conclude that these results illustrate the great potential of the C_4 smoothing method as a simulation shortcut. Nevertheless, more simulations for a wide variety of cases and meshes will be necessary to confirm these preliminary conclusions.

Acknowledgments

This work has been partially supported by a postdoctoral fellowship *Beatriu de Pinós* (2006 BP-A 10075) by the *Generalitat de Catalunya*. Reference DNS results have been performed on the IBM MareNostrum supercomputer at the Barcelona Supercomputing Center. The authors thankfully acknowledge this institution.

REFERENCES

[1] P.R. Spalart, Strategies for turbulence modelling and simulations, *Int. J. Heat and Fluid Flow* **21**, 252–263 (2000).

[2] J.L. Guermond, J.T. Oden and S. Prudhomme, Mathematical perspectives on large eddy simulation models for turbulent flows, *J. Math. Fluid Mech.* **6**, 194–248 (2004).

[3] J. Leray, Sur le movement d'un liquide visqueux emplissant l'espace, *Acta Math.* **63**, 193–248 (1934).

[4] A. Cheskidov, D.D. Holm, E. Olson and E.S. Titi, On a Leray-α model of turbulence, *Roy. Soc. London, Proc. Series A, Math. Phys. & Engng. Sci.* **461**, 629–649 (2005).

[5] C. Foias, D.D. Holm and E.S. Titi ES, The Navier-Stokes-alpha model of fluid turbulence, *Physica D* **152**, 505–19 (2001).

[6] S. Stolz and N.A. Adams, An approximate deconvolution procedure for large-eddy simulation, *Phys. Fluids* **11**, 1699–1701 (1999).

[7] B.J. Geurts and D.D. Holm, Regularization modeling for large-eddy simulation, *Phys. Fluids* **15**, L13-16 (2003).

[8] R. Verstappen, On restraining the production of small scales of motion in a turbulent channel flow. *Computers & Fluids* **37** 887–897 (2008).

[9] A.N. Kolmogorov, Dissipation of energy in locally isotropic turbulence, *Dokl. Akad. Nauk SSSR* **32** 19-21 (1941) [in Russian].

[10] A.N. Kolmogorov, The local structure of turbulent motion in an incompressible fluid, *Dokl. Akad. Nauk SSSR* **30** 299-303 (1941) [in Russian].

[11] C. Foias, O. Manley, R. Rosa and R.Teman, Estimates for the energy cascade in three-dimensional turbulent flows, *C.R. Acad. Sci. Paris, Série I* **333** 499-504 (2001).

[12] R. Verstappen, On the inertial range of symmetry-preserving regularization models for turbulent flow, *PAMM* **7**, 1100901-1100902 (2007).

[13] R.W.C.P. Verstappen and A.E.P. Veldman, Symmetry-preserving discretization of turbulent flow, *J. Comp. Phys.* **187** 343–368 (2003).

[14] F. X. Trias, M. Soria, A. Oliva, and C. D. Pérez-Segarra. Direct numerical simulations of two- and three-dimensional turbulent natural convection flows in a differentially heated cavity of aspect ratio 4. *Journal of Fluid Mechanics*, **586** 259–293 (2007).

[15] F. X. Trias, A. Gorobets, M. Soria, and A. Oliva. Direct numerical simulation of a differentially heated cavity of aspect ratio 4 with Ra-number up to 10^{11} - Part I: Numerical methods and time-averaged flow. *International Journal of Heat and Mass Transfer*, **53** 665–673 (2010).

[16] F. X. Trias, A. Gorobets, M. Soria, and A. Oliva. Direct numerical simulation of a differentially heated cavity of aspect ratio 4 with Ra-number up to 10^{11} - Part II: Heat transfer and flow dynamics. *International Journal of Heat and Mass Transfer*, **53** 674–683 (2010).

[17] J. Meyers and P. Sagaut. Is plane-channel flow a friendly case for the testing of large-eddy simulation subgrid-scale models? *Physics of Fluids*, **19** 048105 (2007).

[18] B. Castaing, G. Gunaratne, F. Heslot, L. Kadanoff, A. Libchaber, S. Thomae, X. Wu, S. Zaleski, and G. Zanetti. Scaling of hard thermal turbulence in Rayleigh-Bénard convection. *Journal of Fluid Mechanics*, **204** (1) 1–30 (1989).

[19] Siegfried Grossmann and Detlef Lohse. Scaling in thermal convection: a unifying theory. *Journal of Fluid Mechanics*, **407** 27–56 (2000).

[20] Joël Sommeria. The elusive 'ultimate state' of thermal convection. *Nature*, **398** 294–295 (1999).

[21] Huidan Yu, Ning Li, and Robert E. Ecke. Scaling in laminar natural convection in laterally heated cavities: Is turbulence essential in the classical scaling of heat transfer? *Physical Review E*, **76** 026303 (2007).